Versão do arquivo anexado / Version of attached file:

Versão do Editor / Published Version

Mais informações no site da editora / Further information on publisher's website:
https://ieeexplore.ieee.org/document/7843590

DOI: 10.1109/LCOMM.2017.2664806

Direitos autorais / Publisher's copyright statement:

Co-Channel Interference and Background Noise in κ-μ Fading Channels

Nidhi Bhargav, Carlos Rafael Nogueira da Silva, Young Jin Chun, Simon L. Cotton, and Michel Daoud Yacoub

***Abstract*— In this letter, we derive novel analytical and closed form expressions for the outage probability, when the signal-of-interest (SoI) and the interferer experience κ–μ fading in the presence of Gaussian noise. Most importantly, these expressions hold true for independent and non-identically distributed κ–μ variates, *without* parameter constraints. We also find the asymptotic behaviour when the average signal to noise ratio of the SoI is significantly larger than that of the interferer. It is worth highlighting that our new solutions are very general owing to the flexibility of the κ–μ fading model.**

***Index Terms*— Background noise, co-channel interference, generalized fading distribution, κ-μ fading, outage probability.**

I. Introduction

UNDERSTANDING the performance of systems in the presence of co-channel interference (CCI) is critical for successful system design in many applications such as cellular networks, device-to-device (D2D) and body area networks (BANs). Several authors have dealt with the effects of CCI for different limiting factors [1], [2]. These include different types of fading for the signal-of-interest (SoI) and the interfering links [1], the presence or absence of background noise (BN), and number of independent or correlated interferers [2]. While all of these factors influence the impact of CCI, among the most prevalent are the fading characteristics of the SoI and the CCI links. As these are not always similar, it is important that a flexible model is used to represent the fading observed in both. Among the many fading models proposed, one of the most flexible and important is the κ-μ fading model [3]. It was developed to account for line-of-sight (LOS) channels which may promote the clustering of scattered multipath waves. Most importantly, it includes many of the popular fading models such as the Rice ($\kappa = K$, $\mu = 1$), Nakagami-m ($\kappa \to 0$, $\mu = m$), Rayleigh ($\kappa \to 0$, $\mu = 1$) and One-Sided Gaussian ($\kappa \to 0$, $\mu = 0.5$) as special cases.

The outage probability (OP) is an important performance metric that can be used to characterize the signal to interference ratio in systems with CCI. For generalized fading models, [2], [4], and [5] provide OP analyses when the SoI and the interfering links undergo η-μ/η-μ, η-μ/κ-μ and κ-μ/η-μ fading. These analyses either provide approximate expressions, or consider that μ takes positive integer values for the SoI or the interfering link. Furthermore, Bhargav *et al.* [6] provide an OP analysis over κ-μ/κ-μ fading channels which can be adapted to study interference-limited scenarios.

A plethora of research has been carried out to characterize the performance in the presence of CCI and BN. To the best of the authors' knowledge, none of the prior works have considered the OP performance metric in the presence of BN, when both the SoI and CCI experience κ-μ fading with arbitrary parameters. Motivated by this, we derive novel expressions for the OP in the presence of CCI and BN for independent and non-identically distributed ($i.n.i.d$) κ-μ variates. Due to the flexibility of the κ-μ fading model, these novel formulations unify the OP expressions in the presence of BN, when the SoI and the CCI are subject to Rayleigh, Rice, Nakagami-m and One-Sided Gaussian fading models.

II. The System Model

Consider the system model of a typical wireless communication scenario in the presence of multiple interferers as shown in Fig. 1. Let P_S, P_{I_j} and N_0, represent the transmit power at the source of the SoI (Node S), the transmit power of the jth interfering node and the noise power at the intended receiver (Node D). Then, the instantaneous signal to noise ratio (SNR) at node D is given by $\gamma_S = P_S|h_S|^2/N_0$, while the instantaneous interference-to-noise-ratio (INR) is given by $\gamma_{I_j} = P_{I_j}|h_{I_j}|^2/N_0$. Here, h_S and h_{I_j} represent the complex fading channel gain for the SoI and the jth interfering channel, respectively. The OP of the signal-to-interference-plus-noise-ratio (SINR) in the presence of CCI and BN is defined as

$$P_{OP}(\gamma_{th}) = \mathbb{P}\left(\gamma_S \leqslant \left(\gamma_{I_j} + 1\right)\gamma_{th}\right). \tag{1}$$

Let us assume that the SoI and the interferer are both subject to κ-μ fading. The probability density function (pdf) and the cumulative distribution function (cdf) of the instantaneous SNR, γ, for a κ-μ fading channel can be obtained from [3, eq. (10)] and [3, eq. (3)], where $\kappa > 0$ is the ratio of the total power of the dominant components to that of the scattered waves in each of the clusters, $\mu > 0$ is the number of multipath clusters, $\bar{\gamma} = \mathbb{E}(\gamma)$, is the average SNR where $\mathbb{E}(\cdot)$ denotes the expectation, $I_\nu(\cdot)$ is the modified Bessel function of the first kind with order ν [7, eq. (9.6.10)] and $Q_\cdot(\cdot,\cdot)$ is the generalized Marcum Q-function. We consider the channel components of the SoI and the interfering links with parameters $\{\kappa_S, \mu_S, \bar{\gamma}_S\}$ and $\{\kappa_{I_j}, \mu_{I_j}, \bar{\gamma}_{I_j}\}$, respectively.

III. Outage Probability Analysis

Let us denote the set of interfering nodes as Φ and assume $M = |\Phi|$ nodes are randomly deployed in the network, where $|\mathcal{A}|$ represents the cardinality of set $\mathcal{A}$. Based on (1), the OP for multiple interferers is given as follows

$$\mathbb{E}_G\left[\mathbb{P}\left(\gamma_S \leq \gamma_{th}\left(G+1\right)\right)\Bigg|\sum_{j\in\Phi}\gamma_{I_j} = G\right]. \tag{2}$$

Manuscript received December 15, 2016; revised January 10, 2017; accepted February 1, 2017. Date of publication February 3, 2017; date of current version May 6, 2017. This work was supported by the U.K. Engineering and Physical Sciences Research Council under Grant Reference EP/L026074/1 and by CNPq under Grant Reference 304248/2014-2. The associate editor coordinating the review of this letter and approving it for publication was J. Zhang.

N. Bhargav, Y. J. Chun, and S. L. Cotton are with the Wireless Communications Laboratory, Institute of Electronics, Communications and Information Technology, Queen's University of Belfast, Belfast BT3 9DT, U.K. (e-mail: nbhargav01@qub.ac.uk; y.chun@qub.ac.uk; simon.cotton@qub.ac.uk).

C. R. N. da Silva and M. D. Yacoub are with the Wireless Technology Laboratory, School of Electrical and Computer Engineering, University of Campinas, Campinas 13083-970, Brazil (e-mail: carlosrn@decom.fee.unicamp.br; michel@decom.fee.unicamp.br).

Digital Object Identifier 10.1109/LCOMM.2017.2664806

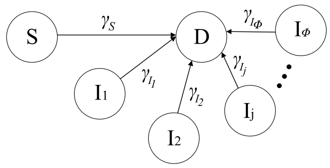

Fig. 1. The proposed system model.

For the multiple interfering scenario depicted in Fig. 1, we consider that the interferers contribute CCI components which undergo independent and identically distributed ($i.i.d$) fading whereas the CCI components and the SoI are $i.n.i.d$ RVs. Capitalizing on the fact that the sum of $i.i.d$ κ-μ power RVs is another κ-μ power RV with appropriately chosen parameters, i.e., G is a κ-μ power RV with parameters $\{\kappa_I, M\mu_I, M\bar{\gamma}_I\}$, an analytical expression for the OP can be obtained as[1]

$$P_{OP}(\gamma_{th}) = \sum_{n=0}^{\infty}\sum_{i=0}^{\mu_S+n}\frac{C_S}{g_{in}}\left(\mathcal{K}_S\gamma_{th}\right)^{\mu_S+n}\mathbb{E}\left[G^i\right] \tag{3}$$

where $C_S = (-1)^n L_n^{(\mu_S-1)}(\kappa_S\mu_S)e^{-\kappa_S\mu_S}$, L_p^{λ} is the generalized Laguerre polynomial [7, eq. (22.5.54)] of degree p and order λ, $\mathcal{K}_t = \mu_t(1+\kappa_t)/\bar{\gamma}_t$ with t being the appropriate index, $g_{in} = \Gamma(i+1)\,\Gamma(\mu_S+n-i+1)$, $\Gamma(\cdot)$ is the Gamma function, M denotes the number of interferers and $\mathbb{E}\left[G^i\right]$ is the ith moment of G. The proof of (3) is given in Appendix A.

Substituting for $\mathbb{E}\left[G^i\right]$ from [8] and performing the mathematical manipulations in Appendix A, we obtain (4), shown at the bottom of this page. Here, $C_{i,n} = (-1)^{-i+n} L_{-i+n}^{(\mu_S-1)}(\kappa_S\mu_S)e^{-\kappa_S\mu_S}$, $C_I = (-1)^n L_n^{(M\mu_I-1)}(M\kappa_I\mu_I)\, e^{-M\kappa_I\mu_I}$, $p_1 = n+\mu_S$, $p_2 = i+\mu_S$ and $U(\cdot,\cdot,\cdot)$ is the confluent Tricomi hypergeometric function [7, eq. (13.1.3)].

A closed form expression for the OP is given by

$$P_{OP}(\gamma_{th}) = \frac{e^{-\kappa_S\mu_s}}{e^{M\kappa_I\mu_I}}\mathbf{H}[\mathbf{x}_M; (\alpha_M, \mathbf{A}); (\beta_M, \mathbf{B}); \mathcal{L}] \tag{5}$$

where $\mathbf{H}[\cdot;\cdot;\cdot;\cdot]$ denotes the Fox H-function on several variables [9, eq. (1.1)], $\mathcal{L}$ is an infinite contour in the complex space, $\mathbf{x}_M = \left[\gamma_{th}\mathcal{K}_S, -\gamma_{th}\kappa_S\mu_s\mathcal{K}_S, \mathcal{K}_I, -M\kappa_I\mu_I\mathcal{K}_I\right]$, $\alpha_M = [0,0,0,\mu_S,0,M\mu_I,0]$ and $\beta_M = [1,0,\mu_S,M\mu_I]$;

$$\mathbf{A} = \begin{pmatrix} -1 & -1 & 0 & 0\\ 0 & 0 & -1 & -1\\ 1 & 1 & 1 & 1\\ 1 & 0 & 0 & 0\\ 0 & 1 & 0 & 0\\ 0 & 0 & 1 & 0\\ 0 & 0 & 0 & 1 \end{pmatrix};\quad \mathbf{B} = \begin{pmatrix} -1 & -1 & 0 & 0\\ 1 & 1 & 0 & 0\\ 0 & -1 & 0 & 0\\ 0 & 0 & 0 & -1 \end{pmatrix}$$

From the residue theorem [10], [11], the Fox H-function in (5) may be implemented as the sum of residues simplified as (4). See Appendix B for proof.

[1]It is noteworthy that (3) works for the $i.n.i.d$ case but within some range of the parameters which, unfortunately, we have not been able to specify yet. On the other hand, our main results, namely (4) and (5) are well consolidated.

Furthermore, considering the special case when the interferers are subject to Nakagami-m fading i.e., letting $\kappa_I \to 0$ and $\mu_I = m_I$ in the first expression of (4) we obtain

$$P_{OP}(\gamma_{th}) = \sum_{n=0}^{\infty}\frac{C_S}{\Gamma(1+p_1)}\left(\frac{\mathcal{K}_S\gamma_{th}\bar{\gamma}_I}{m_I}\right)^{p_1} \times U\left(n-\mu_S, 1-p_1-Mm_I, \frac{m_I}{\bar{\gamma}_I}\right) \tag{6}$$

where m_I represents the well-known Nakagami parameter m for the interfering channel; C_S, $\mathcal{K}_S$ and p_1 are as defined before. We now find the asymptotic behavior for the general case, (4), when the average SNR of the SoI is signficantly larger than that of the interferer[2] via Lemma 1.

Lemma 1: For $\frac{\bar{\gamma}_S}{\bar{\gamma}_I} \gg 1$, the OP of the SINR converges to the following asymptotic expression

$$\lim_{\frac{\bar{\gamma}_S}{\bar{\gamma}_I}\to\infty} P_{OP}(\gamma_{th}) = \frac{e^{-\kappa_S\mu_S-M\kappa_I\mu_I}}{\Gamma(1+\mu_S)}\left(\frac{\gamma_{th}\mathcal{K}_S}{\mathcal{K}_I}\right)^{\mu_S} \times \sum_{n=0}^{\infty}\frac{(M\kappa_I\mu_I)^n}{n!}\,U\left(-\mu_S, 1-n-\mu_S-M\mu_I, \mathcal{K}_I\right), \tag{7}$$

which can be further simplified given that the interferers are subject to Nakagami-m fading as follows

$$\lim_{\frac{\bar{\gamma}_S}{\bar{\gamma}_I}\to\infty} P_{OP}(\gamma_{th}) = \frac{e^{-\kappa_S\mu_S}}{\Gamma(1+\mu_S)}\left(\frac{\gamma_{th}\bar{\gamma}_I\mathcal{K}_S}{m_I}\right)^{\mu_S} \times U\left(-\mu_S, 1-\mu_S-Mm_I, \frac{m_I}{\bar{\gamma}_I}\right). \tag{8}$$

Proof: See Appendix C. ■

IV. Numerical Results

For the figures presented here, $\gamma_{th} = 0$ dB. Fig. 2 depicts the OP versus $\bar{\gamma}_S$ for a different number of interfering signals and for two sets of $\{\kappa_S, \kappa_I\}$ and $\{\mu_S, \mu_I\}$. We observe that as $\bar{\gamma}_S$ increases the OP decreases for each M. However, the rate at which the OP decreases is lower when κ_S is small. In all cases, the analytical results agree with the simulations. It is worth highlighting that even with an efficient method of simulation [12] for non-integer values of κ and μ, the formulations compute as quickly and in the region of very low probability the formulas are much faster than simulation.[3]

Fig. 3 shows the variation in OP versus $\bar{\gamma}_S$ when $M = 1$. We observe that in the low SNR region, the OP is barely affected

[2]For example, in systems using interference suppression techniques which successfully constrain the interference power to be much less than the SoI.

[3]We note that due to the definition of the κ-μ fading model, for the particular case when μ takes an integer value, simulation is naturally faster due to the straightforward combination of the underlying Gaussian variates.

$$P_{OP}(\gamma_{th}) = \begin{cases} \displaystyle\sum_{n=0}^{\infty}\sum_{i=0}^{n}\frac{C_{i,n}\,(M\kappa_I\mu_I)^i}{g_{in}e^{M\kappa_I\mu_I}}\left(\frac{\mathcal{K}_S\gamma_{th}}{\mathcal{K}_I}\right)^{-i+p_1} U\left(i-p_1, 1-p_1-M\mu_I, \mathcal{K}_I\right), & \dfrac{\gamma_{th}\mathcal{K}_S}{\mathcal{K}_I} < 1\\ \displaystyle 1-\frac{e^{-\gamma_{th}\mathcal{K}_S}}{e^{\kappa_S\mu_S}}\sum_{n=0}^{\infty}\sum_{i=0}^{\infty}\frac{C_I\,(\kappa_S\mu_S)^i}{i!\,\Gamma(p_2)}\left(\frac{\mathcal{K}_I}{\gamma_{th}\mathcal{K}_S}\right)^{n+M\mu_I} U\left(1-p_2, 1-p_2-n-M\mu_I, \gamma_{th}\mathcal{K}_S\right), & \dfrac{\gamma_{th}\mathcal{K}_S}{\mathcal{K}_I} > 1 \end{cases} \tag{4}$$

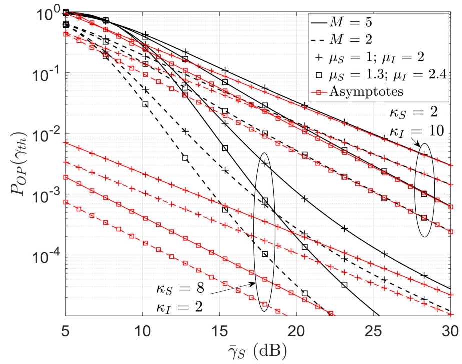

Fig. 2. OP versus $\bar{\gamma}_S$ for an increasing number of interfering signals. $\{\kappa_S, \kappa_I\} = \{2, 10\}$, $\{\kappa_S, \kappa_I\} = \{8, 2\}$, $\bar{\gamma}_I = 1$ dB and $\gamma_{th} = 0$ dB. Black lines represent analytical results, black markers represent simulation results and red lines represent asymptotic results.

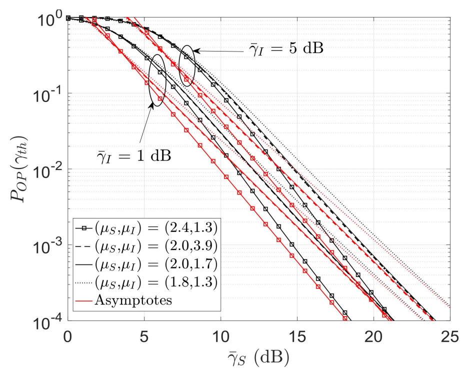

Fig. 3. OP versus $\bar{\gamma}_S$ for a range of μ_S and μ_I. Here $M=1$, $\kappa_S=2$, $\kappa_I=10$, $\gamma_{th} = 0$ dB and $\bar{\gamma}_I = \{1, 5\}$ dB. Red lines represent asymptotic results.

by μ_S. For increasing $\bar{\gamma}_S$ (medium to high SNR region), the OP decreases as μ_S increases with the rate of decay occurring faster for higher values of μ_S.

V. Conclusion

We derived novel expressions for the OP in the presence of CCI and BN for arbitrary parameters. Both single and multiple interfering scenarios are considered and extensive simulations are presented, which agree with the analytical results. Finally, it is worth highlighting that the results presented here will find immediate use in emergent wireless applications such as D2D communications and BANs, both of which are susceptible to CCI and BN caused by inter-tier and intra-tier interferences (in the case of D2D), and other co-located wearable devices (in the case of BANs). Given that transmission via dominant and scattered signal paths is often an inherent characteristic of both D2D [13] and BAN [14] communications, the versatility of the κ-μ fading model will be extremely beneficial for fully understanding the role of interference in determining system performance for these applications.

Appendix A
Proof of Equation (3) and (4)

An analytical solution for (2) can be derived by using the generalized Marcum Q-function in [15, eq. (2.6)] for non-negative real parameters a, b and υ. Substituting this in the κ-μ cdf and using the resultant expression in (2), followed by applying the binomial series identity to the relavant bracketed term, we obtain (3). Substituting for $\mathbb{E}\left[G^i\right]$ from [8] we obtain

$$P_{OP}(\gamma_{th}) = \sum_{n=0}^{\infty}\sum_{i=0}^{\mu_S+n} \frac{C_S (M\mu_I)^{(i)}\, {}_1F_1\left(M\mu_I + i; M\mu_I; M\kappa_I\mu_I\right)}{g_{in} e^{M\kappa_I\mu_I} \left(\mathcal{K}_S\gamma_{th}\right)^{-\mu_S-n} \mathcal{K}_I^i} \tag{9}$$

where C_S and g_{in} are as defined before, $x^{(p)} = \frac{\Gamma(x+p)}{\Gamma(x)}$ is the Pochhammer symbol and ${}_1F_1(\cdot\,\cdot, \cdot)$ is the confluent hypergeometric function. Replacing the confluent hypergeometric function with its series form [16, 07.20.02.0001.01], changing the order of summation and summing on index i, we obtain

$$P_{OP}(\gamma_{th}) = \sum_{m=0}^{\infty}\sum_{n=0}^{\infty} \frac{C_S \left(M\kappa_I\mu_I\right)^m \left(\mathcal{K}_S\gamma_{th}\right)^{\mu_S+n} \mathcal{K}_I^{m+M\mu_I}}{e^{M\kappa_I\mu_I} m!\Gamma\left(\mu_S+n+1\right)} \times U\left(m+M\mu_I, 1+m+n+M\mu_I+\mu_S, \mathcal{K}_I\right). \tag{10}$$

Now substituting $U(a, b, z) = z^{1-b} U(a-b+1, 2-b, z)$ [16, 07.33.17.0007.01], and changing the order of summation using the third identity of the infinite double sum [17], we obtain the first expression in (4) that converges for $\gamma_{th}\mathcal{K}_S/\mathcal{K}_I < 1$.

Replacing the confluent Tricomi hypergeometric function [16, 07.33.06.0002.01] and the generalized Laguerre polynomial [16, 05.02.02.0001.01] with their series representations in (10), we obtain (11), as shown at the top of the next page. Here, $p_3 = m + M\mu_I$ and

$$\mathcal{C}_{mi} = \frac{\left(\kappa_S\mu_S\right)^i \left(M\kappa_I\mu_I\right)^m}{e^{\kappa_S\mu_S + M\kappa_I\mu_I} m!};\ \mathcal{G}_1 = \frac{\Gamma(p_1)}{\Gamma(1+p_1)\,\Gamma(p_2)\,\Gamma(1-i+n)},$$
$$\mathcal{G}_2 = \frac{\Gamma\left(-p_3-p_1\right)(p_3)^{(k)}}{\Gamma\left(-p_1\right)\left(1+p_3+p_1\right)^{(k)}};\ \mathcal{G}_3 = \frac{\Gamma\left(p_3+p_1\right)(-p_1)^{(k)}}{\Gamma\left(p_3\right)\left(1-p_3-p_1\right)^{(k)}}.$$

Now, summing over index n using the fifth identity of the infinite double sum [17], substituting ${}_1F_1(b-a; b; z) = e^z {}_1F_1(a; b; -z)$ [16, 07.20.17.0013.01], followed by transforming the Gauss hypergeometric function, ${}_2F_1(\cdot\,\cdot; \cdot; \cdot)$, using [18, eq. (7.3.1.6)], and replacing ${}_2F_1(\cdot\,\cdot; \cdot; \cdot)$ with its series form [16, 07.23.02.0001.01] we obtain (12), as shown at the top of the next page, where

$$\mathcal{G}_4 = \frac{\Gamma\left(-p_3-p_2\right)(p_3)^{(k)}}{\Gamma\left(-p_2\right)\Gamma\left(1+p_2\right)\left(1+p_3+p_2\right)^{(k)}};$$
$$\mathcal{G}_5 = \frac{\Gamma\left(n+p_3\right)\Gamma\left(n+p_3+p_2\right)\Gamma\left(-p_3\right)\Gamma\left(1+p_3\right)}{\Gamma\left(1-p_3\right)\Gamma\left(1+n+p_3\right)\Gamma\left(p_2\right)\Gamma\left(p_3\right)^2}.$$

We then substitute $k = n - m$ in the first summation [17] and sum over index m. This is followed by using ${}_1F_1(b-a; b; z) = e^z {}_1F_1(a; b; -z)$ in the second summation, substituting $n = k - m$ [17] and summing the second summation over index m. This simplifies (using the tricomi hypergeometric function [16, 07.33.02.0001.01]) to (13), as shown at the top of the next page. Finally, using $U(a, b, z) = z^{1-b} U(a-b+1, 2-b, z)$ in (13) we obtain the second expression in (4) that converges for $\gamma_{th}\mathcal{K}_S/\mathcal{K}_I > 1$.

$$P_{OP}(\gamma_{th}) = \sum_{m=0}^{\infty}\sum_{n=0}^{\infty}\sum_{k=0}^{\infty}\sum_{i=0}^{n} \frac{(-1)^{n+i}\, \mathcal{C}_{mi}\, \mathcal{G}_1}{i!\; k!} (\gamma_{th}\mathcal{K}_S)^{p_1} \left(\mathcal{G}_2 \mathcal{K}_I^{k+p_3} + \mathcal{G}_3 \mathcal{K}_I^{k-p_1}\right) \tag{11}$$

$$P_{OP}(\gamma_{th}) = 1 + \sum_{m=0}^{\infty}\sum_{k=0}^{\infty}\sum_{i=0}^{\infty} \frac{(-1)^{2i}\, \mathcal{C}_{mi}\, \mathcal{G}_4}{i!\; k!\; e^{\gamma_{th}\mathcal{K}_S}} \mathcal{K}_I^{k+p_3} (\gamma_{th}\mathcal{K}_S)^{p_2}\, {}_1F_1\left(1+k+p_3;\, 1+k+p_2+p_3;\, \gamma_{th}\mathcal{K}_S\right)$$
$$+ \sum_{n=0}^{\infty}\sum_{m=0}^{\infty}\sum_{i=0}^{\infty} \frac{\mathcal{C}_{mi}\, \mathcal{G}_5}{i!\; n!} \left(\frac{-\mathcal{K}_I}{\gamma_{th}\mathcal{K}_S}\right)^{n} \left(\frac{\gamma_{th}\mathcal{K}_S}{\mathcal{K}_I}\right)^{-p_3} {}_1F_1\left(-n-p_3;\, 1-n-p_3-p_2;\, -\gamma_{th}\mathcal{K}_S\right) \tag{12}$$

$$P_{OP}(\gamma_{th}) = 1 - \sum_{n=0}^{\infty}\sum_{i=0}^{\infty} \frac{C_I\, (\kappa_S \mu_S)^i\, \mathcal{K}_I^{n+\mu_I}}{i!\; \Gamma(p_2)\, e^{\kappa_S\mu_S + \gamma_{th}\mathcal{K}_S}} (\gamma_{th}\mathcal{K}_S)^{p_2}\, U\left(1+n+M\mu_I;\, 1+p_2+n+M\mu_I;\, \gamma_{th}\mathcal{K}_S\right) \tag{13}$$

Appendix B
Proof of Equation (5)

A closed form expression for (2) can be obtained by expressing the pdf and cdf of the κ-μ distribution as a double Mellin-Barnes contour integral. The contour integral representation for the κ-μ pdf may be obtained using [16, 01.03.07.0001.01] and [16, 03.02.26.0008.01] which writes the exponential function as a Mellin-Barnes contour integral and the modified bessel function as a Meijer G function which in turn is defined as Mellin-Barnes contour integral as in [16, 07.34.07.0001.01]. A contour integral representation for the κ-μ cdf can be obtained directly from the definition as

$$F_\gamma(\gamma) = e^{-\kappa\mu} \left(\frac{1}{2\pi j}\right)^2 \oint\!\!\oint_{\mathcal{L}} \Phi(x_1, x_2) \times (\gamma\, \mathcal{K})^{-x_1} (-\gamma\, \kappa\, \mu\, \mathcal{K})^{-x_2} \mathrm{d}x_1 \mathrm{d}x_2 \tag{14}$$

with $\mathcal{L}$ being an appropriate contour on the complex space, $j = (-1)^{1/2}$ and

$$\Phi(x_1, x_2) = \frac{\Gamma(-x_1 - x_2)\Gamma(\mu + x_1)\Gamma(x_2)}{\Gamma(1 - x_1 - x_2)\Gamma(\mu - x2)}. \tag{15}$$

Replacing (14) in (2) with the appropriate indexes and using the κ-μ pdf for the interferer as a contour integral, changing the order of integration and using [19, eq. (2.2.4.24)], the result can be interpreted as a multivariable Fox H-function as in (5).

Appendix C
Proof of Lemma 1

We find the asymptotic behaviour of the OP when $\frac{\bar{\gamma}_S}{\bar{\gamma}_I} \gg 1 \implies \frac{\gamma_{th}\mathcal{K}_S}{\mathcal{K}_I} = \frac{\gamma_{th}\mu_S(1+\kappa_S)}{\mu_I(1+\kappa_I)} \frac{\bar{\gamma}_I}{\bar{\gamma}_S} \ll 1$. Rewriting the first expression in (4) as

$$P_{OP}(\gamma_{th}) = \left(\frac{\gamma_{th}\mu_S(1+\kappa_S)\bar{\gamma}_I}{\mu_I(1+\kappa_I)\bar{\gamma}_S}\right)^{\mu_S} \sum_{n=0}^{\infty}\sum_{i=0}^{n} \frac{C_{i,n}\, (M\kappa_I\mu_I)^i}{g_{in} e^{M\kappa_I\mu_I}} \times \left(\frac{\gamma_{th}\mu_S(1+\kappa_S)\bar{\gamma}_I}{\mu_I(1+\kappa_I)\bar{\gamma}_S}\right)^{-i+n} \times U\left(i - p_1, 1 - p_1 - M\mu_I, \frac{(1+\kappa_I)\mu_I}{\bar{\gamma}_I}\right) \tag{16}$$

and setting $i = n$ we obtain (7). Now, considering the special case when the interferers are subject to Nakagami-m fading in (7) we obtain (8), which completes the proof.

References

[1] J. M. Romero-Jerez and A. J. Goldsmith, "Receive antenna array strategies in fading and interference: An outage probability comparison," *IEEE Trans. Wireless Commun.*, vol. 7, no. 3, pp. 920–932, Mar. 2008.

[2] N. Y. Ermolova and O. Tirkkonen, "Outage probability analysis in generalized fading channels with co-channel interference and background noise: $\eta-\mu/\eta-\mu$, $\eta-\mu/\kappa-\mu$ and $\kappa-\mu/\eta-\mu$ scenarios," *IEEE Trans. Wireless Commun.*, vol. 13, no. 1, pp. 291–297, Jan. 2014.

[3] M. D. Yacoub, "The κ-μ distribution and the η-μ distribution," *IEEE Antennas Propag. Mag.*, vol. 49, no. 1, pp. 68–81, Feb. 2007.

[4] J. F. Paris, "Outage probability in $\eta-\mu/\eta-\mu$ and $\eta-\mu/\kappa-\mu$ interference-limited scenarios," *IEEE Trans. Commun.*, vol. 61, no. 1, pp. 335–343, Jan. 2013.

[5] S. Kumar *et al.*, "Analysis of outage probability and capacity for $\kappa-\mu/\eta-\mu$ faded channel," *IEEE Commun. Lett.*, vol. 19, no. 2, pp. 211–214, Feb. 2015.

[6] N. Bhargav *et al.*, "Secrecy capacity analysis over κ-μ fading channels: Theory and applications," *IEEE Trans. Commun.*, vol. 64, no. 7, pp. 3011–3024, Jul. 2016.

[7] M. Abramowitz and I. A. Stegun, "Handbook of mathematical functions with formulas, graphs, and mathematical tables," Dept. Commerce, Nat. Bureau Standards, Washington, DC, USA, Tech. Rep., 1972. [Online]. Available: http://people.math.sfu.ca/~cbm/aands/abramowitz_and_stegun.pdf

[8] N. Y. Ermolova, "Moment generating functions of the generalized η-μ and κ-μ distributions and their applications to performance evaluations of communication systems," *IEEE Commun. Lett.*, vol. 12, no. 7, pp. 502–504, Jul. 2008.

[9] N. T. Hai and H. M. Srivastava, "The convergence problem of certain multiple Mellin-Barnes contour integrals representing H-functions in several variables," *Comput. Math. Appl.*, vol. 29, no. 6, pp. 17–25, Mar. 1995. [Online]. Available: http://www.sciencedirect.com/science/article/pii/089812219500003H

[10] K. Knopp, *Theory of Functions Parts I and II, Two Volumes Bound as One, Part I*. New York, NY, USA: Dover, 1996.

[11] S. G. Krantz, *Handbook of Complex Variables*. Boston, MA, USA: Birkhäuser Basel, 1999.

[12] R. Cogliatti *et al.*, "Practical, highly efficient algorithm for generating κ-μ and η-μ variates and a near-100% efficient algorithm for generating α-μ variates," *IEEE Commun. Lett.*, vol. 16, no. 11, pp. 1768–1771, Nov. 2012.

[13] M. Peng *et al.*, "Device-to-device underlaid cellular networks under rician fading channels," *IEEE Trans. Wireless Commun.*, vol. 13, no. 8, pp. 4247–4259, Aug. 2014.

[14] S. L. Cotton *et al.*, "The κ-μ distribution applied to the analysis of fading in body to body communication channels for fire and rescue personnel," *IEEE Antennas Wireless Propag. Lett.*, vol. 7, pp. 66–69, 2008.

[15] S. András *et al.*, "The generalized Marcum Q- function: An orthogonal polynomial approach," *Acta Univ. Sapientiae Math.*, vol. 3, no. 1, pp. 60–76, 2011.

[16] Wolfram Research, Inc. (2016). *Visited*, accessed on May 18, 2016. [Online]. Available: http://functions.wolfram.com/id

[17] Wolfram Research, Inc. (2016). *General Identities, Visited*, accessed on Sep. 18, 2016. [Online]. Available: http://functions.wolfram.com/GeneralIdentities/12

[18] A. P. Prudinkov *et al.*, *Integrals and Series: More Special Functions*, vol. 3. New York, NY, USA: Gordon and Breach, 1990.

[19] A. P. Prudinkov *et al.*, *Integrals and Series: Elementary Functions*, vol. 1. Moscow, Russia: Taylor & Francis, 2002.